

Bound state spectroscopy of NH–He

Galina Kerenskaya, Udo Schnupf, and Michael C. Heaven

Department of Chemistry, Emory University, Atlanta, Georgia 30322

Ad van der Avoird

Institute of Theoretical Chemistry, NSRIM, University of Nijmegen, Toernooiveld 1, 6525 ED Nijmegen, The Netherlands

(Received 6 August 2004; accepted 31 August 2004)

The NH–He van der Waals complex was characterized via laser excitation of bands associated with the NH $A^3\Pi-X^3\Sigma^-$ transition. It was demonstrated that the ground state supports a bound level with a rotational constant of $B''=0.334(2)$ cm⁻¹. These results are in agreement with the predictions of recent high-level theoretical calculations. Spin–orbit predissociation of the excited complex was observed, and the spectra yield insights regarding the NH(A)+He potential energy surfaces. © 2004 American Institute of Physics. [DOI: 10.1063/1.1808416]

INTRODUCTION

The NH radical has been identified as a promising prototype for studies of ultracold molecules.^{1,2} The large rotational constant and magnetic moment of NH($X^3\Sigma^-$) are well suited for techniques that entail ³He buffer gas loading followed by evaporative cooling in a magnetic trap. For the radicals to remain in the trap it is essential that the cross section for Zeeman relaxation induced by collisions with He be extremely small. This cross-section has not been measured, but theoretical calculations² indicate that it is a factor of at least 10⁵ smaller than the elastic cross section at temperatures in the range of 0.5–1 K. The reliability of this prediction is critically dependent upon the accuracy of the theoretical NH(X)–He potential energy surface. This potential was calculated by Krems *et al.*² and Cybulski *et al.*³ The surface exhibits a shallow minimum at long range that is just deep enough to support a bound state of the NH(X)–He complex. Hence experimental verification of the existence of this complex, and measurement of its rotational constant, provides a test of the quality of the theoretical potential.

Weakly bound radical complexes are most readily characterized using the techniques of electronic spectroscopy. In the present study we have used excitation of bands associated with the NH $A^3\Pi-X^3\Sigma^-$ transition to observe NH–He. Consequently, information concerning the NH($A^3\Pi$)+He interaction is also obtained. Potential energy surfaces for this system have been calculated previously⁴ and used to predict inelastic scattering cross sections for NH(A)+He collisions.⁵ In this Communication we report the first observation of the NH–He complex and use spectroscopic data for the A–X transition to evaluate properties of the *ab initio* potential energy surfaces.

EXPERIMENT

NH–He complexes were formed in a free-jet expansion and detected by laser-induced fluorescence (LIF). The apparatus used for this work has been described previously.⁶ NH radicals were formed in the early stages of the expansion by 193 nm multiphoton dissociation of NH₃. A carrier gas mix-

ture of He with (0.02–0.04)% NH₃ was used to drive the expansion. The gas mixture was expanded through the 0.7 mm orifice of a pulsed valve (General Valve, Series 9), operated at a repetition rate of 10 Hz with a pulse duration of 1.3 ms. Optimal formation of NH(X)–He was observed using a source pressure of 28 atm.

The beam from a pulsed tunable dye laser crossed the expansion approximately 7 mm from the nozzle orifice. For excitation of the NH 1–0 band region, frequency doubling of the laser was used to generate light in the 303–306 nm range. LIF was dispersed by a 0.25 m monochromator and detected by a photomultiplier. The monochromator was used primarily as a band-pass filter. A slit width of 6 mm, corresponding to a band-pass of 12 nm, was used. Typically, the monochromator was set to monitor the NH $A-X^3\Pi_0-0$ or 1–1 emission bands⁷ (near 336 nm).

RESULTS AND ANALYSIS

Searches for bands of the complex were made in the vicinity of the monomer 1–0 and 0–0 transitions. The complex was first detected in a medium-resolution, power-broadened spectrum taken in the region of the 1–0 transition. This spectrum is shown in Fig. 1. The partially resolved complex features are clearly evident in this trace, centered close to the monomer $R_1(1)$ parent line. The source pressure dependence of the intensity of these features were consistent with assignment to the binary complex.

Rotationally resolved spectra for the complex were obtained by reducing the laser power. Figure 2 shows a trace recorded in the vicinity of NH 0–0 $R_1(1)$ line using a source pressure of 28 atm. Note that the $A^3\Pi$ state is inverted, so the $R_1(1)$ transition terminates on the $^3\Pi_2$ component. In Fig. 2 the lines of the complex are interleaved between and overlapped by the lines of the monomer. The species assignment of the complex features was confirmed by observing the effect of the source pressure on the relative intensity. Rotational line assignments for two bands of the complex are indicated in Fig. 2. Figure 3 shows the complex features adjacent to the monomer $^RQ_{21}(1)$ (which accesses the $^3\Pi_1$

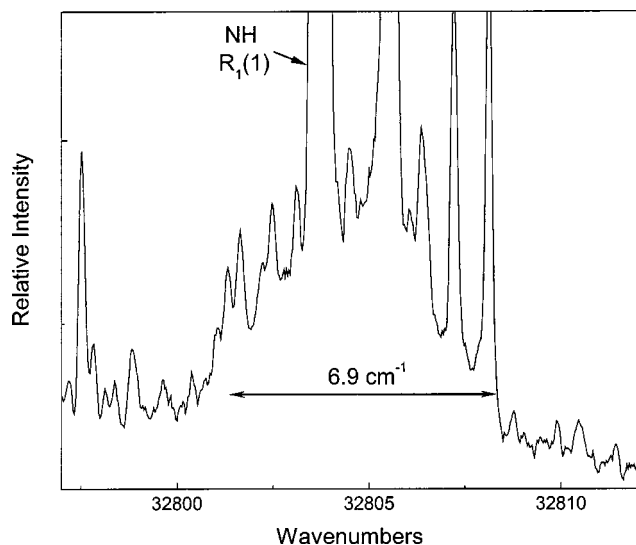


FIG. 1. Medium-resolution spectrum showing the NH-He complex feature associated with the NH $A-X$ 1-0 transition. The intense (off-scale) unlabeled lines are those of the NH monomer.

component of the excited state). At higher energy a broad complex feature was observed approximately 1 cm^{-1} to the high frequency side of the $Q_{31}(1)$ line (not shown in the figure, this transition terminates on the $^3\Pi_0$ component).

Analysis of the NH-He rotational structure was guided by the results from theoretical calculations. The potential energy surface of Cybulski *et al.*³ for the ground state has a well depth of $D_e'' = 19.8\text{ cm}^{-1}$. This minimum occurs at the Jacobi coordinates $R_e = 3.35\text{ \AA}$ and $\theta_e = 62.3^\circ$ (where $\theta = 0^\circ$ for collinear NH-He). Bound state calculations³ for this surface yielded a binding energy of $D_0'' = 4.42\text{ cm}^{-1}$. The predicted rotational energies indicated that the coupling of the electron spin to the rotational motion of the complex would

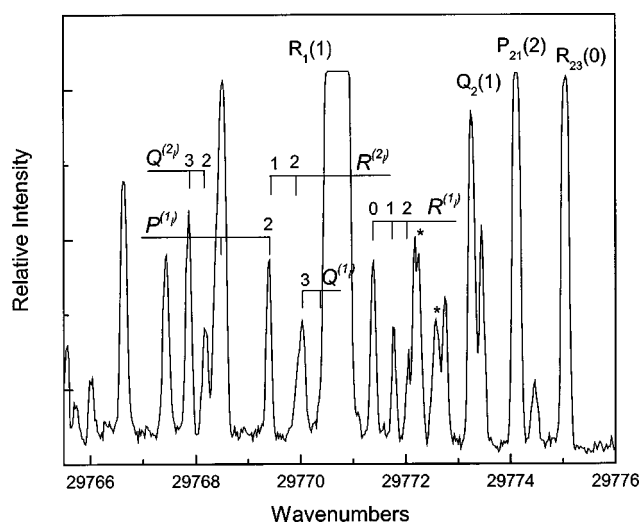


FIG. 2. Rotationally resolved spectrum of NH-He complex features associated with the NH $A^3\Pi_2-X$ 0-0 transition. The rotational lines of the complex are labeled using the l quantum number for the ground state. The features marked by asterisks also appear to be lines of the complex. The most intense line in the center of this trace is a blend of the NH 0-0 band $R_1(1)$ line with the 1-1 band $R_{21}(1)$ line. The other intense unlabeled lines are also from the NH monomer.

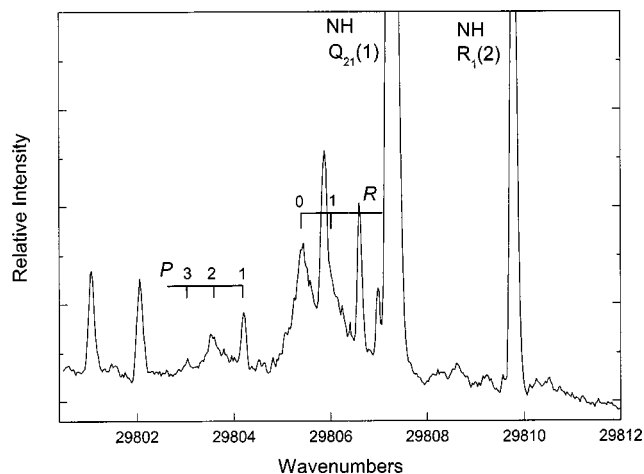


FIG. 3. Rotationally resolved spectrum of NH-He complex features associated with the NH $A^3\Pi_1-X$ 0-0 transition. The rotational lines of the complex are labeled using the l quantum number for the ground state.

be very weak. As a consequence, rotational levels of NH(X)-Ne are very similar to those of analogous closed shell complexes. The end-over-end rotational angular momentum of the entire complex is labeled using the quantum number l . For example, for the $l=1$ level the three spin components (total angular momentum $J=0, 1$, and 2) span an energy range of 0.004 cm^{-1} . Hence the spin splitting is well below the resolution of the present measurements. The stable levels of the complex correlated with non-rotating NH ($n=0, j=1$). Here n represents the total angular momentum of NH excluding the spin (S) and $\mathbf{j}=\mathbf{n}+\mathbf{S}$. The last stable level (in the calculations) is for $l=3$. Fitting the energies for $l=0-2$ to the rigid rotor expression $E''_{\text{Rot}} = B''l(l+1)$ defined a prediction for the effective rotational constant of $B''(\text{calc}) = 0.313\text{ cm}^{-1}$.

New calculations were performed to obtain information concerning the rovibronic structure of NH(A)-He. Potential energy surfaces were generated and used to predict the pattern of bound state energy levels. Details of these calculations will be presented elsewhere.⁸ The equilibrium structure was found to be collinear NH(A)-He ($D_e' = 40\text{ cm}^{-1}$, $R_e = 3.3\text{ \AA}$, and $\theta_e = 0^\circ$), with a secondary minimum for the alternative linear geometry (well-depth 26 cm^{-1} , $R_e = 3.0\text{ \AA}$). These results are in qualitative agreement with the *ab initio* calculations of Jonas and Staemmler,⁴ but the wells are deeper. Jonas and Staemmler⁴ were primarily interested in the repulsive part of the NH(A)-He potential, and noted that their well depth for the NH-He minimum (21 cm^{-1}) was underestimated by a factor of at least two. Rovibronic level calculations with the new potentials predicted that only states correlating with NH $A^3\Pi_2, j=2$ are bound. These states are conveniently described using the quantum label P, which is the unsigned projection of j on the body-fixed axis. The interaction with He splits the NH $j=2$ level into $P = 2_1, 2_u, 1_1, 1_u$ and 0 levels (ascending energy ordering). This splitting is mainly governed by the anisotropy of the potential energy surface. Despite the fact that the A state potential is much deeper than that of the ground state, the calculated binding energy of the complex was found to be

just 3.2 cm^{-1} , with a zero-point rotational constant (derived from the $\langle R^{-2} \rangle$ expectation value) of 0.303 cm^{-1} . The surprisingly large zero-point energy for the A state was a consequence of the pronounced anisotropy of the average potential. This is similar to the situation encountered for He–HF.^{9,10}

Assignment of the observed spectral features was performed by searching for ground state combination differences that were compatible with the theoretical estimate for the rotational constant. The complex band assignments indicated in Fig. 2 were established by this method. Rigid rotor energy level expressions were assumed for the lower [$E''_{\text{ROT}} = B''l(l+1)$] and upper [$E'_{\text{ROT}} = B'J(J+1)$] states. For the upper state J is the total angular momentum of the complex. Fitting to the line positions yielded a common ground state constant of $B'' = 0.334 \pm 0.002 \text{ cm}^{-1}$ for both bands. The upper states yielded rotational constants of $B'(2_1) = 0.306 \pm 0.002 \text{ cm}^{-1}$ and $B'(1_1) = 0.267 \pm 0.002 \text{ cm}^{-1}$. The band origins were displaced from the parent $R_1(1)$ line by -2.4 and 0.2 cm^{-1} , respectively. Additional lines of the complex were observed just above the R -branch head of the 1_1 - X band, but this structure was too fragmentary and overlapped by monomer lines to permit assignment.

The broad features seen in Fig. 3 were clearly associated with the $A^3\Pi_1$ spin-orbit component. The spacing between these peaks is consistent with the $P(2)/R(0)$ assignments shown. Note that there is no Q -branch for this band, indicating that the upper state is $P=0^-$. This is similar to the situation for NH(A)–Ne, where a $P=0^-$ state is also the only level observed for the $^3\Pi_1$ component.¹¹ The linewidths of $P(2)$ and $R(0)$ peaks indicate that the $J=1$ upper state is unstable. The Lorentzian component of this lineshape has a width (HWHM) of 0.17 cm^{-1} , corresponding to a lifetime of 31 ps. A sharp line (instrument limited resolution) is observed in the position where the $P(1)$ line would be expected. However, the $1-1$ band $^RQ_{32}(3)$ line of the monomer is also expected at this position.

Spectra recorded in the region of the NH $1-0$ band were not as well resolved as those taken in the $0-0$ band region due to instrumental limitations. The rotational structures of the 2_1 - X and 1_1 - X transitions were partially resolved. Fitting to these data yielded an estimate for the ground state rotational constant that was consistent with the results from the $0-0$ band data. When the spectra for the $1-0$ and $0-0$ bands were superimposed, the complex lines for the $0-0$ band were centered within the broader lines of the $1-0$ band structure. Hence the rotational constants for the latter were gauged to be indistinguishable (within the error limits) from those derived from the $0-0$ band. The band origins and rotational constants for NH–He are collected in Table I. The larger error ranges for the $1-0$ band constants reflect the lower resolution of the spectrum.

DISCUSSION

The present results demonstrate that NH(X)–He is sufficiently bound to be a stable species at a temperature of approximately 2 K. The rotational constant was the only quantitative property that could be extracted for the ground state.

TABLE I. Band origins and rotational constants for the A - X bands of NH–He.

v^a	ω^b	P	ν_0/cm^{-1c}	B'/cm^{-1c}
0	2	2_1	29768.2(1)	0.306(2)
0	2	1_1	29770.8(1)	0.267(2)
0	1	0^-	29804.7(1)	0.334(12)
1	2	2_1	32801.3(3)	0.306(15)
1	2	1_1	32803.8(2)	0.267(15)

Ground state rotational constant:

Value derived from the $v'=0$ bands, $B''=0.334(2)$.

Value derived from the $v'=1$ bands, $B''=0.334(15)$.

^aVibrational state of NH(A).

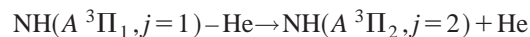
^bProjection of the electronic angular momentum on the N–H axis.

^cEstimates of the $1-\sigma$ errors for the last digit are given in parentheses.

The value obtained was larger than the effective rotational constant derived from the theoretical calculations of Cybulski *et al.*³ Average bond distances, estimated from the relationship $\langle R^{-2} \rangle^{-1/2} = \sqrt{\hbar^2/2\mu B}$ were 4.08 \AA (theory) and 4.00 \AA (obs), which suggests that R_e may be slightly overestimated by the *ab initio* calculations. This would be consistent with the commonly encountered trend for van der Waals interactions where theory overestimates R_e and underestimates D_e .

The spectra do not yield dissociation energies, but the difference between the lower and upper state D_0 values is defined by the displacement of the lowest energy complex band from the monomer parent transition. As noted above, for the NH $0-0$ transition the displacement for the band origin was -2.4 cm^{-1} . If we assume that the theoretical value of $D'_0 = 4.4 \text{ cm}^{-1}$ is a lower bound, this displacement defines a lower bound of $D'_0 > 5.0 \text{ cm}^{-1}$ for the excited state (including the rotational energy for $J'=2$). The A state potential energy surfaces, when scaled to approximate this result, yielded rotation constants that were in reasonable agreement with experiment. However, from preliminary tests it appears that the depth of the *ab initio* potential needs to be increased, while the modulation depth of the anisotropy should be slightly reduced. A modest anisotropy is indicated by the small energy interval between the 2_1 and 1_1 states. Refinement of the A state potentials is in progress.

Lifetime broadening of the NH($A^3\Pi_1$)–He features indicates that the spin-orbit predissociation process



is relatively facile. This is similar to the behavior predicted for CO($a^3\Pi$)–He.¹² The magnitude of the spin-orbit coupling constant for CO(a) (41.45 cm^{-1}) is comparable to that of NH(A) (-34.62 cm^{-1}), and the predicted predissociation lifetimes for the rovibronic levels of CO($a^3\Pi_1$)–He were in the range from 10–700 ps. Spin-orbit predissociation of NH($A^3\Pi_1$)–He is also consistent with the inelastic scattering data for NH(A)+He. Neitsch *et al.*⁵ noted that collisional transfer from $^3\Pi_1$ to $^3\Pi_2$ is rigorously forbidden in the limit of Hund's case (a) coupling, but observable due to the intermediate coupling of NH(A). Even the lowest angular momentum states of NH(A) deviate significantly from the case

(a) limit. For example, the state that is nominally $^3\Pi_2$, $j = 2$ is, in terms of pure case (a) basis functions, given by the superposition $0.899|^3\Pi_2\rangle - 0.412|^3\Pi_1\rangle - 0.150|^3\Pi_0\rangle$. Predissociation of the complex shows that this degree of mixing, with additional contributions resulting from the anisotropy of the interaction potential, is sufficient to induce rapid $^3\Pi_1 \rightarrow ^3\Pi_2$ transfer.

ACKNOWLEDGMENT

Support of this work by the National Science Foundation under Grant No. CHE-0213313 is gratefully acknowledged.

¹S. Y. T. van de Meerakker, R. T. Jongma, H. L. Bethlem, and G. Meijer, *Phys. Rev. A* **64**, 041401/1 (2001).

²R. V. Krems, H. R. Sadeghpour, A. Dalgarno, D. Zgid, J. Kłos, and G. Chałasinski, *Phys. Rev. A* **68**, 051401/1 (2003).

³H. Cybulski, R. V. Krems, H. R. Sadeghpour, A. Dalgarno, J. Kłos, G. C. Groenenboom, A. van der Avoird, D. Zgid, and G. Chałasinski, *J. Chem. Phys.* (to be published).

⁴R. Jonas and V. Steamlar, *Z. Phys. D* **14**, 143 (1989).

⁵L. Neitsch, F. Stuhl, P. J. Dagdigian, and M. H. Alexander, *J. Chem. Phys.* **104**, 1325 (1996).

⁶M. C. Heaven, *Annu. Rev. Phys. Chem.* **43**, 283 (1992).

⁷C. R. Brazier, R. S. Ram, and P. F. Bernath, *J. Mol. Spectrosc.* **120**, 381 (1986).

⁸G. Kerenskaya, U. Schnupf, M. C. Heaven, and A. van der Avoird (unpublished).

⁹C. M. Lovejoy and D. J. Nesbitt, *J. Chem. Phys.* **93**, 5387 (1990).

¹⁰R. Moszynski, B. Jeziorski, A. van der Avoird, and P. E. S. Wormer, *J. Chem. Phys.* **101**, 2825 (1994).

¹¹G. Kerenskaya, U. Schnupf, M. C. Heaven, and A. van der Avoird (to be published).

¹²W. B. Zeimen, G. C. Groenenboom, and A. van der Avoird, *J. Chem. Phys.* **119**, 131 (2003); W. B. Zeimen, G. C. Groenenboom, and A. van der Avoird, *ibid.* **119**, 141 (2003).